Acta Biochim Biophys Sin xxxx, xx(x): xx-xx
https://cstr.cn/32197.14.abbs.2026040
https://doi.org/10.3724/abbs.2026040
Original Article

Original Article

Sulforaphane promotes mammary epithelial cell proliferation in Xizang sheep by increasing FOXM1 and PI3K-Akt signaling

Zhenzhen Zhang[1,†], Tingxian Chen[1,†], Yangzong Zhaxi[2,3], Jiacuo Jinmei[4], Wangjie Zhaxi[5], Quzhu Yixi[6], Zhen Yang[4], Wangsheng Zhao[1,*], and Tianzeng Song[2,*]

[1]College of Life Sciences and Agri-forestry, Southwest University of Science and Technology, Mianyang 621000, China, [2]Institute of Animal Science, Xizang Academy of Agricultural and Animal Husbandry Science, Lhasa 850009, China, [3]Key Laboratory of Animal Genetics and Breeding on Xizang Plateau, Ministry of Agriculture and Rural Affairs, Lhasa 850009, China, [4]Xizang Animal Husbandry Station, Lhasa 850000, China, [5]The Service Station of Agricultural and Animal, Husbandry Technical of Baingoin County, Nagqu 852599, China, and [6]Cultural Service Center of Maqian Township, Baingoin County, Nagqu 852599, China

[†]These authors contributed equally to this work.

*Correspondence address. E-mail: wangshengzhao01@163.com (W.Z.); songtianzeng123@sina.com (T.S.)

Received 1 September 2025 Accepted 10 December 2026 Published 21 May 2026

Abstract

Mammary epithelial cells (MECs) are crucial for milk synthesis and secretion, and their abundance and activity directly influence milk yield and quality. This study investigates the effects of sulforaphane (SFN) on MECs isolated from Xizang Sewa sheep. The findings reveal that SFN at a concentration of 5 μM promotes cell proliferation, enhances DNA synthesis, facilitates the G1/S phase transition, and increases the expression levels of critical cell cycle regulators such as *Ki67*, *PCNA*, *CDK4*, *CCNE1*, *CCNA2*, and *CCND2*. RNA-sequencing analysis further confirms the modulation of numerous genes involved in cell cycle regulation, including *FOXM1*. Further investigation into *FOXM1* demonstrates that its inhibition results in a significant reduction in the mRNA and protein levels of various cell cycle regulatory genes induced by SFN, including *Ki67*, *PCNA*, *CDK4*, and *CCNE1*. Furthermore, treatment with a PI3K-Akt signaling inhibitor (LY294002) leads to a decrease in PI3K-Akt signaling activity, concomitant with reduced levels of *PCNA* and *FOXM1*. However, these effects are ameliorated following SFN treatment. These findings suggest that SFN may significantly enhance cell proliferation of MECs in sheep by upregulating *FOXM1* expression and activating the PI3K-AKT signaling pathway. This study identifies a promising pharmacological target for augmenting milk production in sheep.

Key words sulforaphane, mammary epithelial cells, proliferation, *F0XM1*, PI3K-AKT signaling, Xizang sheep

Introduction

Milk serves as a vital source of nourishment for newborns, providing a diverse array of nutrients essential for their growth and development. In the context of lambs, the successful development of both the animals and the economic outcomes for farmers are closely tied to the lactation capabilities of ewes. The level of mammary gland development directly influences the volume and composition of milk produced by ewes [1]. Within the mammary gland, mammary epithelial cells (MECs) in the acinar glands are the functional units responsible for milk production [2]. MECs are the primary site for milk synthesis and secretion, undergoing iterative processes of proliferation, differentiation, and apoptosis to facilitate milk production [3]. Research indicates that the viability and quantity of MECs directly impact milk yield and quality [4]. Furthermore, MECs are responsive to hormonal signals, such as estrogen and progesterone, contributing to mammary gland development [5]. Therefore, MECs have emerged as a valuable experimental model for investigating the mechanisms of mammary lactation in contemporary research.

Sulforaphane (SFN) is a naturally occurring compound derived from the hydrolysis of thioglycosides and is commonly found in the *Brassica* family [6]. Research has demonstrated that SFN exhibits

© The Author(s) 2026. This is an open access article distributed under the terms of the Creative Commons Attribution-NonCommercial-NoDerivs License (https://creativecommons.org/licenses/by-nc-nd/4.0/).

potential therapeutic effects in improving blood glucose levels, lipid profiles, and oxidative stress [7]. In addition, emerging evidence suggests that SFN may be effective in the treatment of various mental disorders, including Alzheimer's disease, autism spectrum disorder, depression, and schizophrenia [8]. With the in-depth study of plant active ingredients, sulforaphane has received more attention from biomedical researchers.

Studies have shown that SFN has the ability to regulate cell cycle progression at different stages of development. In lung cancer cells, SFN can lead to G0/G1 phase arrest through the depolarization of mitochondrial membrane potential and intracellular reactive oxygen species production [9]. Additionally, SFN has been found to cause G2/M phase arrest in human ovarian cancer cells by downregulating cyclin dependent kinase (*CDK*) 1 and dissociating cyclin B1/CDK1 complexes [10], as well as in prostate cancer cells by decreasing cell viability and inducing G2/M phase arrest [11], and thus exerting anticancer properties. Moreover, SFN has been shown to decrease the proliferation and viability of lens cells [12], reduce cell viability, and impede cell proliferation of human conjunctival fibroblasts [13], while also promoting the proliferation of porcine satellite cells [14]. These studies indicate that SFN acts as a modulator of the cell cycle and proliferation through intricate regulatory pathways.

Nonetheless, limited research has been conducted on the impact of SFN on ovine MECs. In this study, we isolated MECs from the mammary tissue of Sewa sheep and aimed to investigate the effects of SFN on the proliferation of ovine MECs and the underlying molecular mechanisms.

Materials and Methods

Ethics statement

The procedures and handling protocols adhered to the guidelines and regulations approved by the Animal Ethics Committee of Southwest University of Science and Technology (L2022023) and Xizang Autonomous Region Academy of Agriculture and Animal Science (TAS-2022-0008).

Ovine MECs isolation and culture

In a sterile laboratory setting, tissue samples were collected from the mammary glands of healthy lactating Sewa sheep located at Xizang and subjected to a series of procedures. The tissue was first washed with a solution of penicillin and streptomycin in phosphate-buffered saline (PBS) and then dissected into small 1 mm^3 fragments following removal of any surrounding connective tissue. The tissue fragments were then treated with 0.25% type I collagenase (Solarbio, Beijing, China) and incubated at 37°C for 1.5 h with agitation, followed by centrifugation at 200 *g* for 5 min. The resulting cell pellet was then transferred to a culture dish and maintained in growth medium at 37°C with 5% CO_2. The growth medium consisted of 90% DMEM/F12 medium (Gibco, Waltham, USA), 10% fetal bovine serum (Epizyme, Shanghai, China), 5 mM sodium acetate (Sinopharm, Shanghai, China), 5 mg/L hydrocortisone (Solarbio), 5 μg/mL insulin (Sigma, St Louis, USA), 10 kU/L penicillin/streptomycin (Gibco), and 10 ng/mL epidermal growth factor (Pepro, Cranbury, USA).

The growth medium was aspirated once the cells reached 80% confluence and rinsed with PBS. Subsequently, the cells were treated with 0.25% trypsin (Solarbio) at 37°C for 1 min, the enzymatic reaction was halted by the addition of growth medium, and the fibroblasts were removed. The remaining cells were washed twice with PBS before fresh growth medium was added for continued cultivation. Following 2–3 repetitions, relatively pure MECs were obtained. Upon reaching 80% confluence, the purified MECs were washed with PBS and treated with 0.25% trypsin at 37°C for 4 min, and the growth medium was used to stop the digestion. The suspension was collected and centrifuged to remove the supernatant, and the remaining MECs were subcultured into new culture dishes. MECs have been previously identified using common markers for epithelial cell characterization, namely, cytokeratin 7 and 8, as reported in prior studies [15].

Cell viability assay

MECs were seeded in 96-well plates at a concentration of 2×10^3 cells per well. Following cell adhesion, MECs were exposed to varying concentrations (0, 5, 10, 20, and 40 μM) of sulforaphane (SFN; MedChem Express, Princeton, USA) dissolved in dimethyl sulfoxide (DMSO; Solarbio). Subsequently, at time points of 0, 6, 12, 18, 24, 32, 38, 42, and 48 h, the medium in each well was replaced by 100 μL fresh growth medium and 10 μL CCK8 kit (Beyotime, Haimen, China) and then incubated in a cell culture incubator for 2 h. The absorbance at a wavelength of 450 nm was measured using a microplate reader (Flash, Shanghai, China). Data from wells containing only medium without cells were used for background correction. Each treatment group was conducted in 6 replicates.

MECs treatment

To examine the functions of forkhead box M1 (*FOXM1*), MECs were transfected with small interfering RNA (siRNA) following established protocols [16]. Briefly, cells were plated on culture dishes and maintained in growth medium. Upon reaching 30% confluence, cells were transfected with siRNAs targeting *FOXM1* (siRNA1: 5'-GCUCGCCUAGCCACAGCAAGUU-3', siRNA2: 5'-CCAUACUCCUACAUGGCCCUU-3', siRNA3: 5'-ACCCUAGGCCCAAGAAGUCCUU-3'), or a negative control siRNA (NC: 5'-ACCCUCCUCCUACUGCAUCAUU-3') using the transfection reagent GP-transfect-Mate (Gemma, Shanghai, China) as per the manufacturer's guidelines. Subsequently, the medium was replaced by fresh medium containing or lacking 5 μM SFN after 6 h. Cell samples were harvested for further analysis after 36 h.

Prior research indicated that a concentration of 10 μM LY294002 (Selleck Chemicals, Houston, USA) was suitable to inhibit the PI3K-Akt signaling pathway [17]. MECs were exposed to either 5 μM SFN or DMSO for a duration of 12 h, followed by the addition of 10 μM LY294002 to the medium for a 24-h treatment period.

RNA extraction and cDNA synthesis

Total RNA was isolated from MECs using RNAiso Plus (Takara, Dalian, China) according to the manufacturer's instructions. RNAiso Plus was added to the MEC pellets, which were vortexed for 5 min and incubated for 5 min at 25°C. Chloroform (1/5 volume of RNAiso Plus) was added, shaken for 15 s, incubated for 3 min, and centrifuged (12,000 *g*, 4°C, 15 min). The upper aqueous phase was transferred to a new tube, equal amounts of isopropanol were added, and the tube was inverted, incubated for 10 min, and centrifuged (12,000 *g*, 4°C, 10 min). The supernatant was discarded, the pellet was washed with 75% ethanol (DEPC-treated water), centrifuged (7500 *g*, 4°C, 5 min), air-dried, and dissolved in DEPC water. The quality and quantity of the total RNA were assessed using a

NanoDrop spectrophotometer (Thermo, Wilmington, USA). Then, cDNA synthesis was performed utilizing a PrimeScript™ RT reagent Kit with gDNA Eraser (Takara).

RNA-sequencing (RNA-seq)

The treated Xizang sheep MECs were harvested, and total RNA was extracted. RNA quality was assessed using a NanoDrop and an Agilent 2100 system for RNA sequencing. The RNA-seq analyses were conducted by MetWare Biotechnology (Wuhan, China) on an Illumina NovaSeq 6000 platform (Illumina, San Diego, USA). The samples were divided into two groups, DMSO and SFN treatment groups, with 5 biological replicates per group. The data were analyzed as previously reported [18], involving the processing of raw data through in-house Perl scripts. Gene expression quantification was carried out using HTSeq (v0.9.1), while DESeqR (v1.18.0) was utilized for the analysis of differentially expressed genes (DEGs) at the criteria of $|\log2FoldChange| \geq 1$ and a false discovery rate (FDR) < 0.05. Additionally, ClusterProfiler (v4.6.0) was employed for GO and KEGG enrichment analysis.

Quantitative real-time PCR (qPCR)

The specific primers of cell proliferation-related genes were designed using Primer-BLAST, and the primer sequences we used are listed in Supplementary Table S1. The relative mRNA levels of these genes were evaluated by quantitative real-time PCR using TB Green® Premix Ex Taq™ II (Tli RNaseH Plus) (Takara). Amplification was performed according to the manufacturer's instructions under the following thermal cycling conditions: initial denaturation at 95°C for 30 s; 40 cycles of denaturation at 95°C for 5 s and annealing/extension at 60°C for 30 s; followed by a final dissociation stage consisting of 95°C for 15 s, 60°C for 1 min, and 95°C for 15 s. Relative mRNA levels were calculated using the $2^{-\Delta\Delta Ct}$ method and normalized to the 18S rRNA as an internal reference gene.

Flow cytometric analysis

The treated cell samples were collected after digestion. Precipitation was achieved by placing the suspensions in centrifuge tubes and spinning at 300 *g* for 5 min. The resulting cells were then washed with PBS and centrifuged to eliminate any remaining FBS and trypsin. Next, the MECs were fixed in 70% pre-cooled ethanol and incubated at 4°C for 30 min. The supernatant was discarded after recentrifugation, and the cells were washed with PBS. The precipitated MECs were resuspended in 500 μL of PBS and incubated with 20 g/mL RNase A for 30 min at 37°C. MECs were then pelleted by centrifugation, resuspended in 500 μL PBS, and subsequently treated with a 50 g/mL propidium iodide (PI) dyeing solution (Beyotime). The resulting cell suspensions were chilled on ice and incubated for 30 min before being analyzed via flow cytometry. FCS Express software was utilized for data analysis.

EdU staining

Staining was conducted with a BeyoClick™ EdU Kit (Beyotime) in adherence to the guidelines provided by the manufacturer. Briefly, the samples underwent a 4 h incubation in growth medium containing 10 μM EdU, followed by a 15 min fixation in 4% paraformaldehyde at room temperature and three PBS washes. Subsequently, the cells were treated with 0.3% Triton X-100 for 15 min and rinsed with PBS. A 50-μL click reaction solution was then introduced into each well of a 96-well plate, incubated for 30 min, and washed with PBS. Finally, nuclear staining was achieved using Hoechst 33342. The stained samples were visualized using a fluorescence microscope (Nikon, Tokyo, Japan) and analyzed with ImageJ software.

Western blot analysis

Protein samples were extracted from the treated MECs and subjected to western blot analysis using standard protocols. Briefly, proteins were extracted from treated MECs using RIPA lysis buffer, followed by centrifugation at 12,000 *g* for 15 min at 4°C to collect the supernatant. The protein concentration was determined using a BCA assay (Beyotime). The protein samples were mixed with 5× loading buffer and denatured by boiling at 100°C for 10 min. Equal amounts of protein were loaded onto 10% SDS-PAGE gels, separated by electrophoresis, and then transferred onto PVDF membranes. The membranes were blocked with 5% skim milk in TBST for 2 h at room temperature, incubated with primary antibodies overnight at 4°C, washed three times with TBST, and subsequently incubated with secondary antibodies for 2 h at room temperature. Immunoreactive bands were visualized using ECL reagent (Beyotime), and signal intensities were quantified using Image Lab software. Primary antibodies against Ki67 (ab16667), PCNA (ab29), Cyclin E1 (ab33911), β-actin (ab8226), and FOXM1 (ab207298) were purchased from Abcam (Cambridge, UK), while antibodies against PI3K (4257), p-PI3K (17366), Akt (9272), and p-AKT (9271) were purchased from Cell Signaling Technology (Danvers, USA). The secondary antibody from Baoshen (Beijing, China) were employed for protein expression detection.

Statistical analysis

All data are presented as the mean ± standard error of the mean (SEM) and were analyzed with GraphPad Prism 8 software. The unpaired Student's *t* test was used when two groups were compared, and a one-way analysis of variance (ANOVA) was used when three or more groups were compared. Differences were considered significant when the threshold was $P < 0.05$.

Results

A low dose of SFN stimulates the growth of ovine MECs

While SFN has been suggested to play a crucial role in the proliferation of various cell types [14], its specific effect on ovine MECs is not well understood. In this study, MECs were treated with different concentrations of SFN to investigate its impact on cellular viability. The results indicated that there was no significant difference in cell activity between the Blank group and the DMSO group (Figure 1A). High concentrations (20 and 40 μM) of SFN were found to have toxic effects on MECs, leading to a significant reduction in cell activity (Figure 1A). SFN (10 μM) initially had no significant effect on cellular viability, which decreased after 42 h (Figure 1A). In contrast, the administration of 5 μM SFN resulted in a significant increase in the cellular activity of MECs ($P < 0.01$, Figure 1A). In addition, the cell growth curve indicated that treatment with 5 μM SFN led to a stimulation of cell growth starting at 12 h ($P < 0.01$), which eventually reached a plateau after 36 h ($P < 0.001$, Figure 1B). Consequently, based on these findings, a duration of 36 h with 5 μM SFN was chosen for further investigation.

SFN promotes the cell cycle transformation and cell proliferation of MECs

To validate the impact of SFN on cell proliferation, MECs were subjected to pre-treatment with either 5 μM SFN or DMSO for a duration of 36 h. The EdU staining kit was utilized to quantify the number of positive cells, indicative of DNA replication activity. Our results indicated no notable difference between the DMSO group and the Blank group, whereas a significant increase in the number of positive cells was observed following SFN treatment ($P < 0.001$, Figure 2A). In addition, the treated MECs were stained with PI, and flow cytometry was employed to assess the distribution of cells in the G0/G1, S, and G2/M phases of the cell cycle. The results revealed that DMSO did not impact the distribution of cells in different phases of the cell cycle, while the proportion of cells in the S phase was significantly increased in the SFN group (Figure 2B). Our findings demonstrate that SFN has a notable stimulatory effect on DNA synthesis.

Moreover, qPCR analysis revealed a significant upregulation of the transcriptional levels of cell cycle regulatory factors, including *Ki67*, Proliferating Cell Nuclear Antigen (*PCNA*), *CDK4*, *Cyclin E1 (CCNE1)*, *CCNA2*, and *CCND2*, by SFN treatment ($P < 0.001$), while no significant change was observed in the mRNA level of *CDK6* (Figure 3A). Western blot analysis further confirmed the increased posttranscriptional levels of Ki67, PCNA, and CCNE1 following SFN treatment ($P < 0.05$, Figure 3B), suggesting that SFN has the potential to enhance cell proliferation in MECs.

RNA-seq analysis of SFN regulating MEC functions

RNA-seq analysis was utilized to investigate the regulation of the MEC transcriptome by SFN. The SFN group exhibited 521 DEGs compared to the DMSO group (|log2 FoldChange| ≥ 1, FDR < 0.05), with 199 upregulated and 322 downregulated genes (Figure 4A). Subsequent qPCR analysis confirmed that the altered mRNA levels of BUB1 mitotic checkpoint serine/threonine kinase (*BUB1*), cell

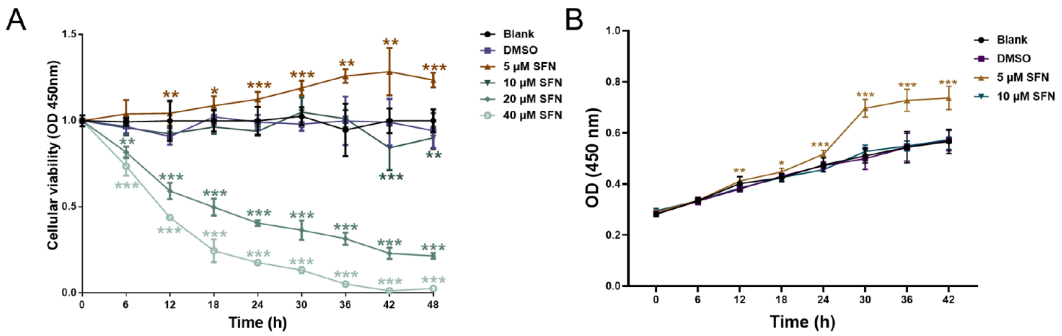


Figure 1. A low dose of SFN stimulates the growth of ovine MECs MECs were treated with various concentrations (0, 5, 10, 20, and 40 μM) of SFN. (A) Cell activity was detected with a CCK8 kit every 6 h. (B) The cell growth curve of MECs was also detected after 0, 5, and 10 μM SFN treatment. Data are presented as the mean ± SEM and were analyzed with ANOVA. $^{*}P < 0.05$, $^{**}P < 0.01$, $^{***}P < 0.001$, $n = 6$.

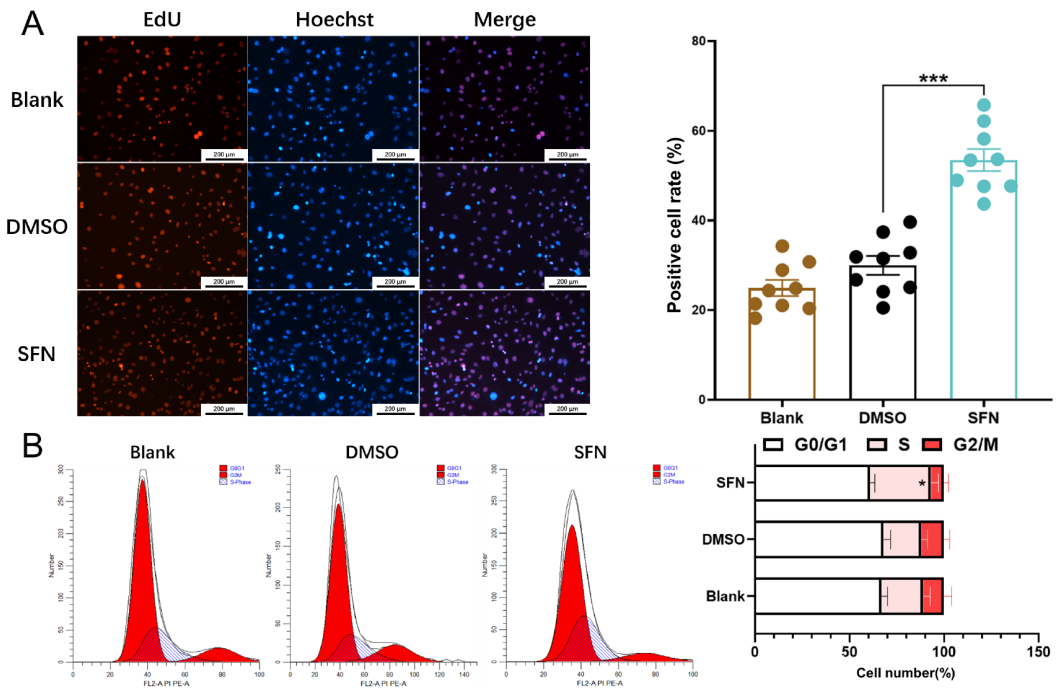


Figure 2. SFN increases DNA synthesis in MECs MECs were exposed for 36 h to 5 μM SFN or DMSO. (A) The MECs were stained with EdU, and the number of EdU-positive cells was measured with a fluorescence microscope. (B) Cell cycle changes were detected by flow cytometry after PI staining. Data are presented as the mean ± SEM and were analyzed with ANOVA. $^{*}P < 0.05$, $^{***}P < 0.001$, $n \geq 3$.

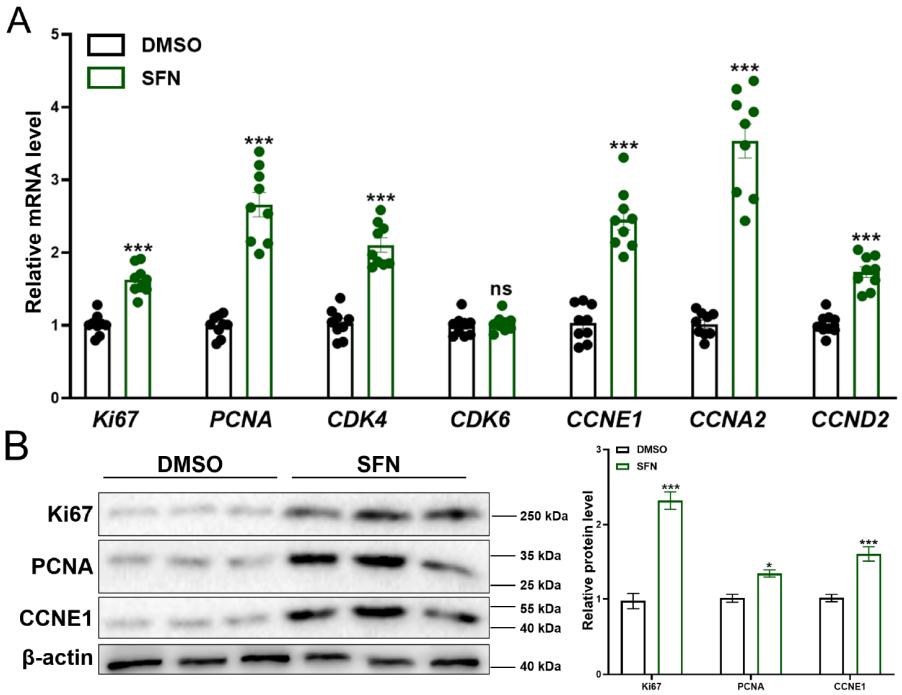


Figure 3. SFN regulates the levels of cell cycle regulatory factors in MECs MECs were pretreated with DMSO or 5 μM SFN for 36 h, and mRNA and protein samples were collected for further analysis. (A) qPCR was used to measure the relative mRNA levels of *Ki67, PCNA, CDK4, CCNE1, CCNA2,* and *CCND2*. (B) Western blot analysis was utilized to detect the protein levels of Ki67, PCNA and CCNE1. Data are presented as the mean ± SEM and were analyzed with unpaired Student's *t* test. $^{*}P < 0.05$, $^{***}P < 0.001$, $n \geq 3$.

division cycle 45 (*CDC45*), cell division cycle associated 2 (*CDCA2*), E2F transcription factor 1 (*E2F1*), minichromosome maintenance complex component 2 (*MCM2*), DNA topoisomerase II alpha (*TOP2A*), forkhead box M1 (*FOXM1*), cyclin dependent kinase inhibitor 1C (*CDKN1C*), calcium voltage-gated channel subunit alpha1 H (*CACNA1H*), F-box protein 32 (*FBXO32*), cysteine dioxygenase type 1 (*CDO1*), thrombospondin 2 (*THBS2*), serpin family F member 1 (*SERPINF1*) and basic helix-loop-helix family member e41 (*BHLHE41*) were consistent with the RNA-seq results (Figure 4B). GO analysis revealed significant enrichment of DEGs in processes closely related to cell proliferation, such as DNA recombination, cell cycle phase transition, DNA replication, cell cycle checkpoint, and DNA duplex unwinding (Figure 4C). KEGG enrichment analysis indicated a significant enrichment in pathways related to DNA replication and the cell cycle. In addition, the enrichment of carbon metabolism and pentose phosphate pathways was observed, indicating their role in energy provision, as well as the enrichment of purine and pyrimidine metabolism for the supply of essential raw materials necessary for DNA replication (Figure 4D). RNA-seq analysis further revealed that SFN treatment modulated a considerable number of cell cycle-regulated genes, such as Wnt family member 10B (*WNT10B*), fibroblast growth factor 18 (*FGF18*), E2F transcription factor 8 (*E2F8*) and factor 7 (*E2F7*) (Figure 4E), suggesting a beneficial regulatory effect of SFN on cell cycle regulation in MECs.

SFN increases the proliferation of MECs by enhancing FOXM1

RNA-seq identified the upregulation of FOXM1 after SFN treatment (Figure 4B,E). FOXM1 is a proliferation-related transcription factor and cell cycle regulator that is widely expressed in proliferating cells [19]. FOXM1 can control G1/S phase and G2/M phase transition through transcriptional activation of cell cycle-related genes [20], thereby regulating cell cycle progression and cell proliferation. Therefore, we attempted to explore the roles of *FOXM1* in SFN promotion of MEC proliferation. The siRNAs targeting *FOXM1* were synthesized and transfected into proliferative MECs. siRNA2 exhibited a remarkable inhibition efficiency of 80.01%, resulting in the *FOXM1* mRNA level being reduced to 19.99% of that in the NC group (Figure 5A). Consequently, siRNA2 was chosen as siFOXM1 for subsequent investigation. Western blot analysis further confirmed that siFOXM1 significantly suppressed the protein levels of FOXM1 (Figure 5B). Furthermore, following transfection with siFOXM1, MECs were treated with SFN for 36 h, after which samples were collected to assess the changes in mRNA and protein levels of proliferation-related factors. The results demonstrated that SFN treatment notably elevated the mRNA levels of *Ki67*, *PCNA*, *CDK4*, *CCNE1*, and *FOXM1*, as shown in previous data (Figure 3A,4B). However, *FOXM1* blockade led to a substantial weakening in the mRNA levels of these genes ($P < 0.01$, Figure 5C). Similarly, protein analysis also revealed that SFN-induced increases in FOXM1, Ki67, and PCNA were reversed upon siFOXM1 treatment (Figure 5D). Flow cytometry indicated a significant decrease in S phase cells following *FOXM1* inhibition despite increased SFN exposure (Figure 5E). These findings suggested that SFN promotes MEC proliferation by targeting FOXM1.

The involvement of the PI3K-Akt signaling pathway in SFN-induced enhancement of MECs proliferation

The abundance of PI3K-Akt signaling, which regulates the function of a wide range of proteins involved in cell growth, proliferation, motility, and cell death [21], was observed following SFN treatment

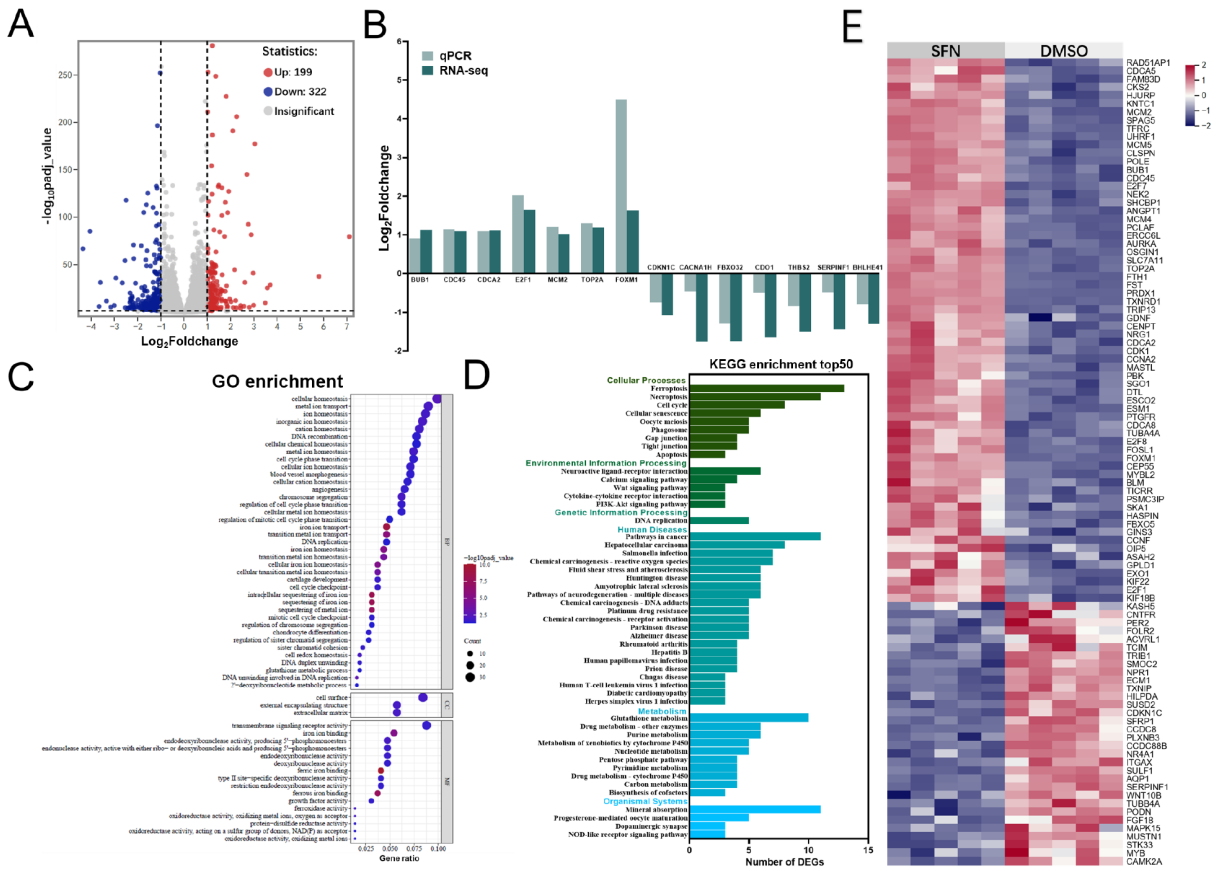


Figure 4. RNA-seq analysis of SFN regulating MEC functions RNA-seq was performed after SFN treatment in MECs. (A) The DEGs were identified following the conditions of |log2FoldChange| ≥ 1 and FDR < 0.05 and are presented as a volcano plot. (B) qPCR was employed to verify the mRNA levels of *BUB1, CDC45, CDCA2, E2F1, MCM2, TOP2A, FOXM1, CDKN1C, CACNA1H, FBXO32, CDO1, THBS2, SERPINF1,* and *BHLHE41.* (C,D) GO and KEGG enrichment analyses were conducted for DEGs. (E) The cell cycle-related genes were selected for heatmap analysis. Data were analyzed with an unpaired Student's *t* test. $n = 5$.

(Figure 4D). This finding aligns with our earlier findings that 5 μM SFN significantly enhances MECs viability (Figure 1) and upregulates proliferation-related markers such as *PCNA* at both the mRNA and protein levels (Figure 3), collectively indicating SFN's pro-proliferative effect. Therefore, we next verified the roles of PI3K-Akt signaling in SFN-promoting MECs proliferation. A concentration of 10 μM LY294002 was applied for 24 h to inhibit the PI3K-Akt signaling pathway. EdU staining revealed a significant decrease in MECs growth following LY294002 treatment. Conversely, the addition of SFN reversed the suppression of MECs proliferation (Figure 6A). Western blot analysis revealed a significant decrease in p-PI3K and p-AKT levels following treatment with LY294002, followed by an increase upon the addition of SFN (Figure 6B). Moreover, the protein levels of PCNA and FOXM1, previously shown to be upregulated by SFN, were also decreased after blocking PI3K-Akt signaling and subsequently increased after SFN addition (Figure 6B). These results, integrated with our prior observations, demonstrated that SFN promotes MEC proliferation by enhancing the PI3K-Akt signaling pathway.

Discussion

SFN has been demonstrated to be a promising regulator of the cell cycle in various cell types [22]. The proliferation of MECs in sheep contributes to enhanced milk production [23]. Therefore, SFN was utilized to treat MECs isolated from sheep mammary tissue, and it was found that SFN significantly promoted MEC proliferation by upregulating the *FOXM1* and PI3K-Akt signaling pathways.

The effects of SFN on cell proliferation and the cell cycle have been extensively investigated in various cell types. SFN influences the cell cycle by modulating the expression and activity of a wide array of genes and proteins involved in cell cycle regulation, including cyclins, CDKs, CDK inhibitors, and checkpoint proteins [24, 25]. In cancer cells, SFN demonstrates the ability to induce cell cycle arrest and promote apoptosis, positioning SFN as a promising candidate for cancer prevention and therapy [26]. However, the specific effects of SFN can vary depending on factors such as cell type, compound concentration, and other cellular components. In non-cancer cells, SFN generally plays a more protective and regulatory role focused on maintaining normal cellular function and safeguarding against damage [27,28], which indirectly supports healthy cell proliferation. Our study revealed that SFN mildly influences sheep MECs primarily by ensuring proper regulation of the cell cycle. Similar to its anti-cancer effects, its promoting effect is dose-dependent. Low doses of SFN modulated the expression of key regulators in the cell cycle, such as cyclins and CDK inhibitors. Consequently, it facilitated progression from G1 phase to S phase in the cell cycle, leading to accelerated proliferation.

FOXM1 is a transcription factor that plays a pivotal role in the

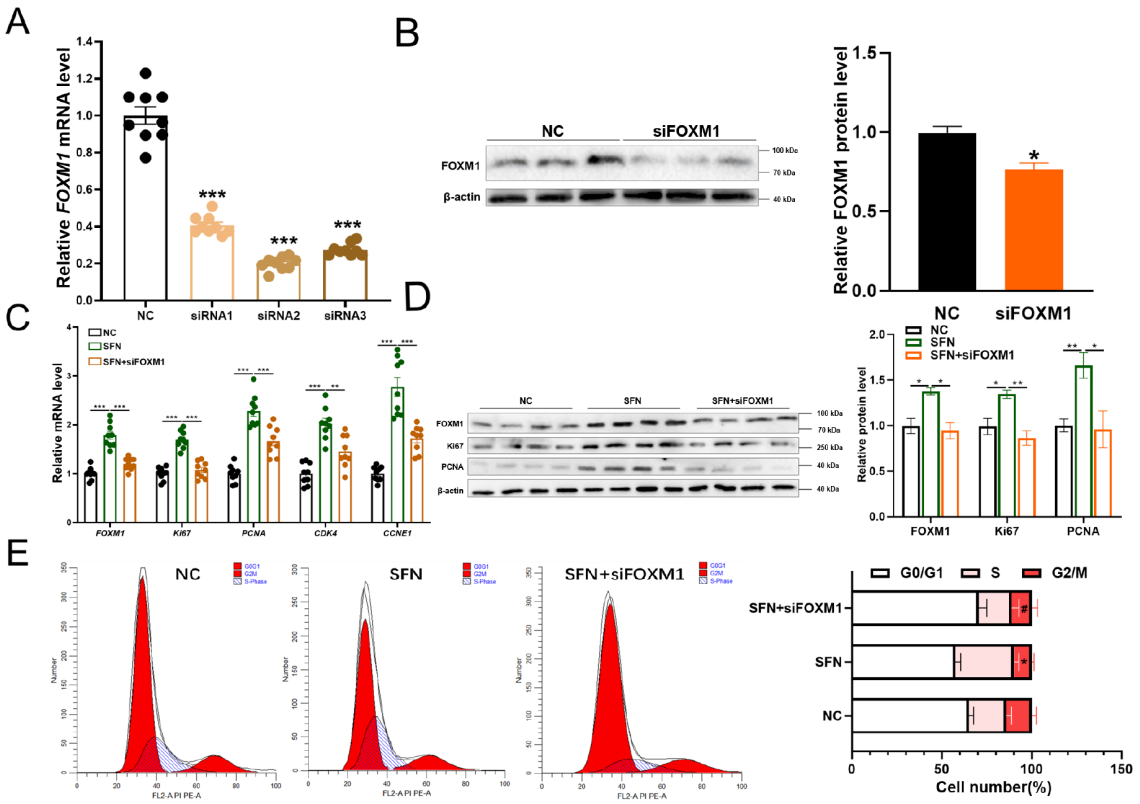


Figure 5. *FOXM1* in SFN increases the proliferation of MECs (A) siRNAs targeting *FOXM1* and siRNA control were synthesized and transfected into proliferative MECs to assess their inhibitory efficiency by qPCR. (B) The protein levels of FOXM1 were evaluated via western blot analysis following transfection with siFOXM1. (C,D) MECs were treated with a control siRNA (NC), SFN combined with the control siRNA (SFN), or SFN in combination with siFOXM1 (SFN + siFOXM1), and the mRNA and protein levels of *FOXM1* and proliferation-related factors were measured by qPCR and western blot analysis. (E) Cell cycle changes were analyzed by flow cytometry. Data are presented as the mean ± SEM, and statistical analysis was performed using unpaired Student's *t* test and ANOVA. $^{*}P < 0.05$, $^{**}P < 0.01$, $^{***}P < 0.001$, *denotes comparison to the NC group; #$P < 0.05$ while # represents comparison to the SFN group in (E). $n \geq 3$.

regulation of the cell cycle, particularly in cell proliferation, differentiation, and survival [19,29]. This regulation is essential for the proper progression of the cell cycle and the maintenance of genomic stability. Studies have demonstrated that FOXM1 regulates the expression of cyclins, such as *CCND1* and *CCNE1* [30], which are critical for the transition from the G1 to the S phase of the cell cycle. *CCND1* activates *CDK4*/*6*, leading to the phosphorylation of the retinoblastoma protein, which subsequently releases *E2F* transcription factors that promotes entry into the S phase [31]. During S phase, *FOXM1* is instrumental in ensuring accurate DNA replication by regulating the expression of genes integral to DNA synthesis and repair, including *CDK1* [32]. Moreover, *FOXM1* has been reported to play a pivotal role in the G2/M transition by upregulating the expression of *PLK1* and *CCNB1*, which are essential for the initiation of mitosis [33]. *FOXM1* facilitates the progression into mitosis by phosphorylating various substrates involved in chromatin condensation, nuclear envelope breakdown, and spindle formation [34]. This regulatory function is crucial for maintaining genomic stability and preventing mutations. Here, we observed that inhibition of *FOXM1* resulted in the suppression of *CDK4*, *CCNE1*, *Ki67*, and *PCNA* expression, which consequently led to a reduction in the number of cells in the S phase. However, the number of cells in the S phase G2/M transition remained unchanged. These discrepancies may be attributable to variations in cell type and state.

Although our research indicated that SFN upregulates *FOXM1* to promote the proliferation of MECs, we acknowledge that the direct mechanistic link between SFN and *FOXM1* has not yet been fully elucidated. Based on the available evidence, we propose that the potential transcriptional and epigenetic mechanisms underlying this regulatory relationship warrant further investigation. In cancer models, SFN has been reported to downregulate *FOXM1* through multiple pathways, including inhibition of *E2F1*-mediated transcription [35], suppression of hyperactivated PI3K-AKT/mTOR signaling [36], and modulation of chromatin accessibility via histone deacetylase (HDAC) inhibition [37], as well as effects on protein degradation and stress responses [38,39]. However, our study reveals a contrasting stimulatory effect of SFN on *FOXM1* in normal MECs, which may be attributed to fundamental differences in regulatory contexts. Unlike cancer cells characterized by dysregulated overexpression of FOXM1 [40], normal MECs maintain tight homeostatic control over FOXM1 levels, thereby creating a permissive environment for SFN-induced upregulation. Our data provide preliminary insights into potential mechanisms in MECs. First, transcriptional regulation via *E2F1*, consistent with RNA-seq results showing SFN-induced upregulation of *E2F1*, may enhance *FOXM1* transcription through E2F1 binding to its promoter. Second, activation of the PI3K-AKT signaling pathway could contribute to *FOXM1* upregulation, either by promoting its transcription via downstream effectors or by stabilizing the FOXM1 protein through

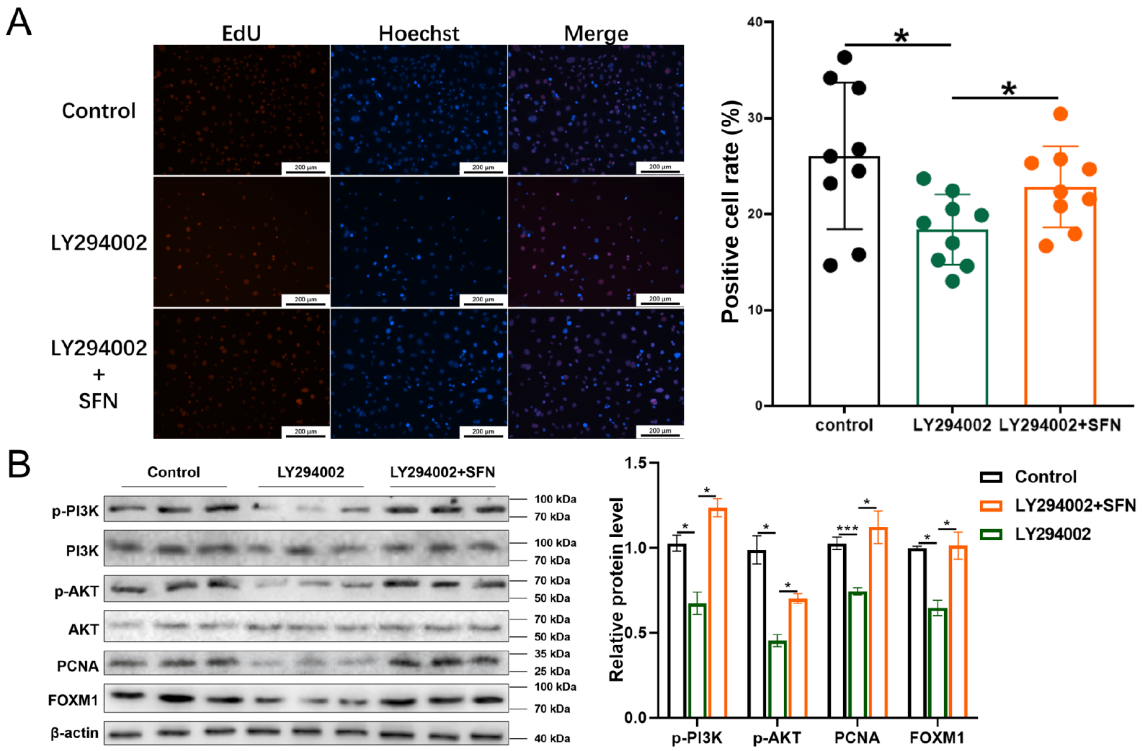


Figure 6. The role of the PI3K-Akt signaling pathway in the SFN-induced cell proliferation of MECs MECs were treated with either 5 μM SFN or DMSO for 12 h, followed by the addition of 10 μM LY294002 for an additional 24 h. (A) The MECs were stained with EdU dye. (B) Western blot analysis was performed to assess the protein levels of p-PI3K, p-AKT, PCNA, and FOXM1. Data are presented as the mean ± SEM and were analyzed with ANOVA. $*P < 0.05$, $***P < 0.001$, $n \geq 3$.

phosphorylation-dependent mechanisms. Additionally, as an HDAC inhibitor, SFN may alter histone acetylation at the FOXM1 locus in MECs, thereby facilitating transcriptional activation, a hypothesis supported by our RNA-seq data, which show enrichment of genes related to chromatin modification. However, these mechanisms need to be further verified.

While our findings indicate that SFN promotes the proliferation of Xizang sheep MECs through FOXM1 and PI3K-Akt signaling, thereby providing a potential mechanistic foundation for enhancing mammary function, several limitations warrant consideration. The current conclusions are derived exclusively from an *in vitro* MEC culture system, which may not fully capture the complexity of the *in vivo* mammary microenvironment. Under physiological conditions, mammary gland development and lactation are regulated by systemic sex hormones, complex intercellular communications, and vascular supply factors—elements that were not represented in the present experimental model. Moreover, it remains unclear whether SFN can be effectively delivered to mammary tissues at concentrations sufficient to activate FOXM1 and PI3K-Akt signaling, a crucial prerequisite for translating *in vitro* observations into *in vivo* applications. Additionally, due to the absence of comprehensive *in vivo* toxicity and safety profiles, the practical feasibility of utilizing SFN as an intervention to enhance milk production remains uncertain. Future studies will focus on addressing these limitations through targeted *in vivo* experiments.

In conclusion, our findings demonstrated that SFN significantly promoted the proliferation of MECs isolated from ovines, potentially through the upregulation of *FOXM1* expression and the activation of the PI3K-AKT signaling pathway. This study elucidated the molecular mechanisms by which SFN influences the proliferation of MECs and identified a promising pharmacological target for enhancing milk production in sheep.

Supplementary Data

Supplementary data are available at *Acta Biochimica et Biophysica Sinica* online.

Data Availability

The raw data were stored in the Sequence Read Archive (SRA) database with accession number PRJNA1020122.

Funding

This work was supported by the grants from the National Natural Science Foundation of China (No. 32260824), a local project guided by the Central Government of Xizang Autonomous Region (Nos. XZ202201YD0007C and XZ202101YD0019C).

Conflict of Interest

The authors declare that they have no conflict of interest.

References

1. Akers RM. A 100-Year Review: mammary development and lactation. *J Dairy Sci* 2017, 100: 10332–10352
2. Slepicka PF, Somasundara AVH, dos Santos CO. The molecular basis of mammary gland development and epithelial differentiation. *Semin Cell Dev Biol* 2021, 114: 93–112
3. Deacon AM, Blouin R, Thibault C, Lacasse P. Mechanism underlying the modulation of milk production by incomplete milking. *J Dairy Sci* 2023,

106: 783–791
4. Dai W, White R, Liu J, Liu H. Organelles coordinate milk production and secretion during lactation: insights into mammary pathologies. *Prog Lipid Res* 2022, 86: 101159
5. Brisken C, Ataca D. Endocrine hormones and local signals during the development of the mouse mammary gland. *WIREs Dev Biol* 2015, 4: 181–195
6. Yagishita Y, Fahey JW, Dinkova-Kostova AT, Kensler TW. Broccoli or sulforaphane: is it the source or dose that matters? *Molecules* 2019, 24: 3593
7. Axelsson AS, Tubbs E, Mecham B, Chacko S, Nenonen HA, Tang Y, Fahey JW, *et al.* Sulforaphane reduces hepatic glucose production and improves glucose control in patients with type 2 diabetes. *Sci Transl Med* 2017, 9: eaah4477
8. Zheng W, Li X, Zhang T, Wang J. Biological mechanisms and clinical efficacy of sulforaphane for mental disorders. *Gen Psychiatry* 2022, 35: e100700
9. Chatterjee S, Rhee YH, Ahn JC. Sulforaphene–carboplatin combination synergistically enhances apoptosis by disruption of mitochondrial membrane potential and cell cycle arrest in human non-small cell lung carcinoma. *J Med Food* 2016, 19: 860–869
10. Chang CC, Hung CM, Yang YR, Lee MJ, Hsu YC. Sulforaphane induced cell cycle arrest in the G2/M phase via the blockade of cyclin B1/CDC2 in human ovarian cancer cells. *J Ovarian Res* 2013, 6: 41
11. Yang SH, Chien CM, Chang LS, Lin SR. Involvement of c-jun N-terminal kinase in G2/M arrest and caspase-mediated apoptosis induced by cardiotoxin III (Naja naja atra) in K562 leukemia cells. *Toxicon* 2007, 49: 966–974
12. Liu H, Smith AJO, Lott MC, Bao Y, Bowater RP, Reddan JR, Wormstone IM. Sulforaphane can protect lens cells against oxidative stress: implications for cataract prevention. *Invest Ophthalmol Vis Sci* 2013, 54: 5236
13. Liu HR. Sulforaphane modulates TGFβ2-induced conjunctival fibroblasts activation and fibrosis by inhibiting PI3K/Akt signaling. *Int J Ophthalmol* 2020, 13: 1505–1511
14. Zhang R, Neuhoff C, Yang Q, Cinar MU, Uddin MJ, Tholen E, Schellander K, *et al.* Sulforaphane enhanced proliferation of porcine satellite cells via epigenetic augmentation of SMAD7. *Animals* 2022, 12: 1365
15. Li R, Pan J, Pan C, Li J, Zhang Z, Shahzad K, Sun Y, *et al.* Transcriptome analysis of mammary epithelial cell between Sewa sheep and East FriEsian sheep from different localities. *BMC Genomics* 2024, 25: 1038
16. Zhang Z, Wu S, Muhammad S, Ren Q, Sun C. miR-103/107 promote ER stress-mediated apoptosis via targeting the Wnt3a/β-catenin/ATF6 pathway in preadipocytes. *J Lipid Res* 2018, 59: 843–853
17. Gu YX, Du J, Si MS, Mo JJ, Qiao SC, Lai HC. The roles of PI3K/Akt signaling pathway in regulating MC3T3-E1 preosteoblast proliferation and differentiation on SLA and SLActive titanium surfaces. *J BioMed Mater Res* 2013, 101A: 748–754
18. Pan C, Li H, Mustafa SB, Renqing C, Zhang Z, Li J, Song T, *et al.* Coping with extremes: the rumen transcriptome and microbiome co-regulate plateau adaptability of Xizang goat. *BMC Genomics* 2024, 25: 258
19. Zheng J, Bu X, Wei X, Ma X, Zhao P. The role of FoxM1 in immune cells. *Clin Exp Med* 2023, 23: 1973–1979
20. Müller GA, Wintsche A, Stangner K, Prohaska SJ, Stadler PF, Engeland K. The CHR site: definition and genome-wide identification of a cell cycle transcriptional element. *Nucleic Acids Res* 2014, 42: 10331–10350
21. Ersahin T, Tuncbag N, Cetin-Atalay R. The PI3K/AKT/mTOR interactive pathway. *Mol BioSyst* 2015, 11: 1946–1954
22. Tsaur I, Thomas A, Taskiran E, Rutz J, Chun FKH, Haferkamp A, Juengel E, *et al.* Concomitant use of sulforaphane enhances antitumor efficacy of sunitinib in renal cell carcinoma *in vitro*. *Cancers* 2022, 14: 4643
23. Rainard P, Gilbert FB, Germon P. Immune defenses of the mammary gland epithelium of dairy ruminants. *Front Immunol* 2022, 13: 1031785
24. Rutz J, Thaler S, Maxeiner S, Chun FKH, Blaheta RA. Sulforaphane reduces prostate cancer cell growth and proliferation in vitro by modulating the cdk-cyclin axis and expression of the cd44 variants 4, 5, and 7. *Int J Mol Sci* 2020, 21: 8724
25. Santos PW, Machado ART, De Grandis R, Ribeiro DL, Tuttis K, Morselli M, Aissa AF, *et al.* Effects of sulforaphane on the oxidative response, apoptosis, and the transcriptional profile of human stomach mucosa cells *in vitro*. *Mutat Res Genet Toxicol Environ Mutagenesis* 2020, 854-855: 503201
26. Gu H, Mao X, Du M. Metabolism, absorption, and anti-cancer effects of sulforaphane: an update. *Crit Rev Food Sci Nutr* 2022, 62: 3437–3452
27. Treasure K, Harris J, Williamson G. Exploring the anti-inflammatory activity of sulforaphane. *Immunol Cell Biol* 2023, 101: 805–828
28. Bernuzzi F, Maertens A, Saha S, Troncoso-Rey P, Ludwig T, Hiller K, Mithen RF, *et al.* Sulforaphane rewires central metabolism to support antioxidant response and achieve glucose homeostasis. *Redox Biol* 2023, 67: 102878
29. Kopanja D, Chand V, O'Brien E, Mukhopadhyay NK, Zappia MP, Islam ABMMK, Frolov MV, *et al.* Transcriptional repression by FoxM1 suppresses tumor differentiation and promotes metastasis of breast cancer. *Cancer Res* 2022, 82: 2458–2471
30. Wierstra I, Alves J. Cyclin E/Cdk2, P/CAF, and E1A regulate the transactivation of the c-myc promoter by FOXM1. *Biochem Biophys Res Commun* 2008, 368: 107–115
31. Anders L, Ke N, Hydbring P, Choi YJ, Widlund HR, Chick JM, Zhai H, *et al.* A systematic screen for CDK4/6 substrates links FOXM1 phosphorylation to senescence suppression in cancer cells. *Cancer Cell* 2011, 20: 620–634
32. Branigan TB, Kozono D, Schade AE, Deraska P, Rivas HG, Sambel L, Reavis HD, *et al.* MMB-FOXM1-driven premature mitosis is required for CHK1 inhibitor sensitivity. *Cell Rep* 2021, 34: 108808
33. Zheng Q, Luo Z, Xu M, Ye S, Lei Y, Xi Y. HMGA1 and FOXM1 cooperate to promote G2/M cell cycle progression in cancer cells. *Life* 2023, 13: 1225
34. Lin TC, Chung PJ, Shen CA, Nguyen TMH, Lin YS, Lin SC, Hsiao SC, *et al.* Depletion of intracellular Ca2+ induces FOXM1 SUMOylation and accumulation on the inner nuclear membrane and accelerates G2/M cell cycle transition. *Eur J Cell Biol* 2023, 102: 151332
35. Millour J, de Olano N, Horimoto Y, Monteiro LJ, Langer JK, Aligue R, Hajji N, *et al.* ATM and p53 regulate FOXM1 expression via E2F in breast cancer epirubicin treatment and resistance. *Mol Cancer Ther* 2011, 10: 1046–1058
36. Tong YX, Zhu SY, Wang ZY, Zhao YX, Saleem MAU, Malh KK, Li XN, *et al.* Sulforaphane ameliorate cadmium-induced blood–thymus barrier disruption by targeting the PI3K/AKT/FOXO1 axis. *J Agric Food Chem* 2024, 72: 13382–13392
37. Tian S, Lei I, Gao W, Liu L, Guo Y, Creech J, Herron TJ, *et al.* HDAC inhibitor valproic acid protects heart function through Foxm1 pathway after acute myocardial infarction. *EBioMedicine* 2019, 39: 83–94
38. Chesnokov MS, Halasi M, Borhani S, Arbieva Z, Shah BN, Oerlemans R, Khan I, *et al.* Novel FOXM1 inhibitor identified via gene network analysis induces autophagic FOXM1 degradation to overcome chemoresistance of human cancer cells. *Cell Death Dis* 2021, 12: 704
39. Su X, Yang Y, Yang Q, Pang B, Sun S, Wang Y, Qiao Q, *et al.* NOX4-derived ROS-induced overexpression of FOXM1 regulates aerobic glycolysis in glioblastoma. *BMC Cancer* 2021, 21: 1181
40. Liao GB, Li XZ, Zeng S, Liu C, Yang SM, Yang L, Hu CJ, *et al.* Regulation of the master regulator FOXM1 in cancer. *Cell Commun Signal* 2018, 16: 57